

Near-threshold resonance in  $e^+e^- \rightarrow \Lambda_c \bar{\Lambda}_c$  processS. G. Salnikov<sup>\*</sup> and A. I. Milstein<sup>†</sup>*Budker Institute of Nuclear Physics, 630090, Novosibirsk, Russia  
and Novosibirsk State University, 630090, Novosibirsk, Russia* (Received 2 October 2023; accepted 5 October 2023; published 27 October 2023)

We discuss the influence of various contributions of the  $\Lambda_c \bar{\Lambda}_c$  potential on the energy dependence of the cross section  $e^+e^- \rightarrow \Lambda_c \bar{\Lambda}_c$  near the threshold. New BESIII experimental data on the cross section and electromagnetic form factors  $G_E$  and  $G_M$  are taken into account. Our predictions are in good agreement with experimental data. We predict a bound state of  $\Lambda_c \bar{\Lambda}_c$  at energy  $\sim 38$  MeV below the threshold that may manifest itself in anomalous behavior of light meson production cross sections in a given energy region.

DOI: 10.1103/PhysRevD.108.L071505

*Introduction.* Currently, much attention has been drawn to the study of processes in which hadrons are produced in  $e^+e^-$  annihilation near the threshold and a strong energy dependence of the cross sections is manifested. For instance, these processes are  $e^+e^- \rightarrow p\bar{p}$  [1–6],  $e^+e^- \rightarrow n\bar{n}$  [7–10],  $e^+e^- \rightarrow B\bar{B}$  [11,12],  $J/\psi(\psi') \rightarrow p\bar{p}\pi^0(\eta)$  [13–15],  $J/\psi(\psi') \rightarrow p\bar{p}\omega(\gamma)$  [15–19],  $e^+e^- \rightarrow \Lambda\bar{\Lambda}$  [20–22],  $e^+e^- \rightarrow \Lambda_c \bar{\Lambda}_c$  [23–25], and  $e^+e^- \rightarrow \phi\Lambda\bar{\Lambda}$  [26]. The energy dependence of the corresponding cross sections can be successfully explained by the interaction of produced hadrons (the final-state interaction) [27–43].

The processes of hadroproduction near the threshold in  $e^+e^-$  annihilation can be described as follows. First, a quark-antiquark pair is produced at small distances  $\sim 1/Q$ , where  $Q$  is the invariant mass of produced particles. Then at distances  $\sim 1/\Lambda_{\text{QCD}}$  a process of hadronization takes place. A system of produced hadrons can be described by some wave function  $\psi(r)$ . Since the relative speed of hadrons near the threshold is small, they interact with each other for quite a long time. As a result, the wave function  $\psi(r)$  differs significantly from that in the case of noninteracting hadrons. In this picture, the amplitude  $T$  of hadroproduction can be represented in the form  $T = T_0 \cdot \psi(0)$ , where  $T_0$  is the amplitude of quark-antiquark pair production at small distances, and  $\psi(0)$  is the wave function of a hadronic system at distances  $r_0 \lesssim 1/\Lambda_{\text{QCD}}$ . Close to the threshold, a characteristic size of the wave function is much larger than  $r_0$ . The amplitude  $T_0$  depends weakly on energy near the

threshold, while the function  $\psi(0)$  has a strong energy dependence. Thus, final-state interaction of hadrons is responsible for the strong energy dependence of the cross section. Note that the specific form of wave functions depends on quantum numbers of produced particles (spin, isospin, orbital angular momentum, etc.). However, the behavior of cross sections near the threshold has some common features.

First of all, we note that the shapes of cross sections near the threshold are approximated not by the usual Breit-Wigner formulas, but the Flatté formulas and their generalizations [44]. These formulas are applicable if there is either a loosely bound state or a virtual state in a system of produced hadrons. In the first case there is a bound state with the energy  $\varepsilon < 0$ ,  $|\varepsilon| \ll |U|$ , where  $U$  is the characteristic value of potential (energy  $\varepsilon$  is counted from the threshold of hadronic pair production). We will call this case a subthreshold resonance. In the second case there is no loosely bound state, but a slight increase of the depth of the potential results in its appearance. In this case we will talk about an above-threshold resonance. In both cases, the modulus of the scattering length  $a$  in the system of produced hadrons is much larger than the characteristic size  $R$  of the potential. For a subthreshold resonance, we have  $a > 0$  and  $\varepsilon = -1/Ma^2$ . In the case of a virtual state we have  $a < 0$ , and the energy of the virtual state by definition is  $\varepsilon = 1/Ma^2 \ll |U|$  (here  $M$  is the mass of the produced hadron). A detailed discussion of this picture can be found in Refs. [38,40].

The Flatté formula is expressed through a small number of parameters (a scattering length, an effective range of interaction) [45]. Therefore, to describe the near-threshold behavior of cross sections we can use any potentials that reproduce the required values of these parameters. The most convenient way to describe near-threshold resonances is using a potential in its simplest form (for example, in the form of a rectangular potential well), finding the

<sup>\*</sup>S.G.Salnikov@inp.nsk.su<sup>†</sup>A.I.Milstein@inp.nsk.su

Published by the American Physical Society under the terms of the [Creative Commons Attribution 4.0 International license](https://creativecommons.org/licenses/by/4.0/). Further distribution of this work must maintain attribution to the author(s) and the published article's title, journal citation, and DOI. Funded by SCOAP<sup>3</sup>.

corresponding wave functions and fitting the parameters of the potential to achieve the best agreement with experimental data. Such approach makes it easy to take into account the Coulomb interaction of produced charged particles, difference in particle masses in the case of several channels, and other specific effects. This approach turned out to be especially convenient for the description of several coupled channels [40].

In this work we use our approach to describe the cross section of  $\Lambda_c \bar{\Lambda}_c$  pair production in  $e^+e^-$  annihilation near the threshold. Experimental data for the cross section of this process were presented in Refs. [23–25]. In the first two papers the cross section of the process was measured, but the data on the electromagnetic form factors were very limited. In a recent paper [25] experimental data for the cross section of the process were obtained with much higher accuracy than in [23,24]. Note that the data on the cross sections in Refs. [23,25] differ noticeably from each other. Also in Ref. [25] the values of electric form factor  $G_E$  and magnetic form factor  $G_M$  of  $\Lambda_c$  were measured. The latter circumstance allows one to reduce significantly the uncertainty of various contributions to the  $\Lambda_c \bar{\Lambda}_c$  interaction potential.

*Theoretical approach.* The approach to the description of the cross section of process  $e^+e^- \rightarrow \Lambda_c \bar{\Lambda}_c$  is similar to the case of  $p\bar{p}$  and  $n\bar{n}$  pair production in  $e^+e^-$  annihilation near the threshold (see Refs. [30,31] and references therein). However, the case of  $\Lambda_c \bar{\Lambda}_c$  pair production is simpler than  $p\bar{p}$  and  $n\bar{n}$  production. Firstly,  $\Lambda_c \bar{\Lambda}_c$  is produced only in the isospin state with  $I = 0$ , in contrast to the case of a nucleon-antinucleon pair which can have isospin  $I = 0$  or  $I = 1$ . In addition, for a nucleon-antinucleon pair it is necessary to take into account the isotopic invariance violation (the proton and neutron mass difference and absence of Coulomb interaction for  $n\bar{n}$  pair). Also, for a nucleon-antinucleon pair it is necessary to take into account the noticeable imaginary part of the optical potential, which takes into account the high probability of pair annihilation into mesons. We have checked that in the case of  $\Lambda_c \bar{\Lambda}_c$  the potential can be considered as a real quantity.

A pair  $\Lambda_c \bar{\Lambda}_c$  produced in  $e^+e^-$  annihilation has quantum numbers  $J^{PC} = 1^{--}$  and the total spin of the system is  $S = 1$ , while the orbital angular momentum  $l$  can be zero or two due to the tensor forces. Thus, the interaction potential of  $\Lambda_c$  and  $\bar{\Lambda}_c$  can be written as ( $\hbar = c = 1$ )

$$\mathcal{V}(r) = -\frac{\alpha}{r} + V_S(r)\delta_{l0} + \left(\frac{6}{Mr^2} + V_D(r)\right)\delta_{l2} + V_T(r)S_{12}. \quad (1)$$

Here  $\alpha$  is the fine-structure constant,  $V_S(r)$  and  $V_D(r)$  are the contributions to the central potentials in  $S$ -wave and  $D$ -wave, respectively,  $V_T(r)S_{12}$  is the tensor potential,

$S_{12} = 6(\mathbf{S} \cdot \mathbf{n})^2 - 4$  is the tensor operator,  $\mathbf{S}$  is the spin operator of the  $\Lambda_c \bar{\Lambda}_c$  pair, and  $\mathbf{n} = \mathbf{r}/r$ . Note that  $V_D(r)$  differs from  $V_S(r)$  due to spin-orbit interaction. Separating the angular and radial variables, we obtain the equations for the radial part  $u(r)$  of the wave function corresponding to the  $S$ -wave, and the radial part  $w(r)$  corresponding to the  $D$ -wave:

$$\left[\frac{p_r^2}{M} + \mathcal{V}(r) - E\right]\Psi(r) = 0, \quad (2)$$

where  $M$  is the mass of the  $\Lambda_c$  baryon,  $E$  is the energy of a pair, counted from the threshold, and  $(-p_r^2)$  is the radial part of the Laplace operator. The wave function  $\Psi(r)$  of the Schrödinger equation (2) has two components, namely,  $\Psi(r) = (u(r), w(r))^T$ . In this basis, the potential  $\mathcal{V}(r)$  can be written in a matrix form

$$\mathcal{V}(r) = \begin{pmatrix} -\frac{\alpha}{r} + V_S & -2\sqrt{2}V_T \\ -2\sqrt{2}V_T & -\frac{\alpha}{r} + \frac{6}{Mr^2} + V_D - 2V_T \end{pmatrix}. \quad (3)$$

The Schrödinger equation (2) has two linearly independent solutions  $\Psi_1(r) = (u_1(r), w_1(r))^T$  and  $\Psi_2(r) = (u_2(r), w_2(r))^T$ , having different asymptotic behavior at large distances; see [37] for more details. Electromagnetic form factors of  $\Lambda_c$  are expressed through these solutions as follows:

$$\begin{aligned} G_E &= \mathcal{G}(u_1(0) - \sqrt{2}u_2(0)), \\ G_M &= \mathcal{G}\left(u_1(0) + \frac{1}{\sqrt{2}}u_2(0)\right). \end{aligned} \quad (4)$$

Here  $\mathcal{G}$  is the amplitude of the  $\Lambda_c \bar{\Lambda}_c$  pair production at small distances. Near the threshold we can consider  $\mathcal{G}$  to be independent of energy. However, in order to describe experimental data in a wider energy region, it is convenient to represent  $\mathcal{G}$  in the form  $\mathcal{G} = \mathcal{G}_0 \cdot F_D(Q)$ , where  $\mathcal{G}_0$  is a constant, and the dipole form factor  $F_D(Q)$  reads

$$F_D(Q) = \frac{1}{\left(1 - \frac{Q^2}{Q_0^2}\right)^2}, \quad Q = 2M + E, \quad Q_0 = 1 \text{ GeV}. \quad (5)$$

It is seen that the ratio  $G_E/G_M$  is independent of  $\mathcal{G}$  and equals

$$\frac{G_E}{G_M} = \frac{u_1(0) - \sqrt{2}u_2(0)}{u_1(0) + \frac{1}{\sqrt{2}}u_2(0)}. \quad (6)$$

Thus, the ratio  $G_E/G_M$  differs from unity only due to the contribution of the  $D$ -wave arising due to tensor forces. At threshold the contribution of the  $D$ -wave is zero so that  $G_E = G_M$ . The integrated cross section of the  $\Lambda_c \bar{\Lambda}_c$  pair production has the form

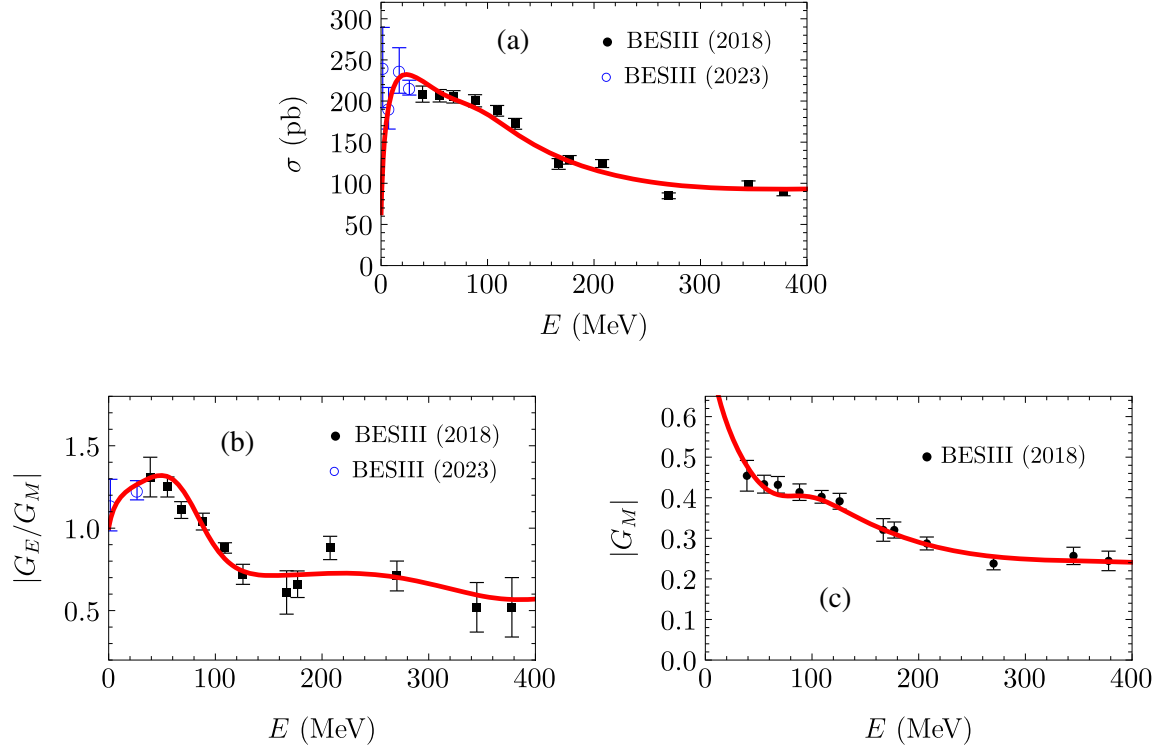


FIG. 1. (a) Cross section of the process  $e^+e^- \rightarrow \Lambda_c \bar{\Lambda}_c$  in the energy region from the threshold to 400 MeV. (b) Ratio of electric and magnetic form factors of the  $\Lambda_c$  baryon. (c) Magnetic form factor. The curves correspond to the predictions of our model. The experimental data are from Refs. [24,25].

$$\sigma = \frac{\pi k \alpha^2}{2M^3} |\mathcal{G}|^2 (|u_1(0)|^2 + |u_2(0)|^2), \quad (7)$$

$$F(r) = \frac{(br)^2}{1 + (br)^2} \quad (9)$$

and its strong energy dependence is determined by the functions  $|u_1(0)|$  and  $|u_2(0)|$ .

It has been pointed out in the Introduction that, to describe near-threshold behavior of the cross section, one can use different shapes of potentials, and the parameters of these potentials can be found by comparing theoretical predictions with experimental data. In our work we choose these potentials in the form of rectangular potential wells

$$V_n(r) = U_n \theta(R_n - r), \quad n = S, D, T, \quad (8)$$

where  $\theta(x)$  is the Heaviside function,  $U_n$  and  $R_n$  are some fitting parameters. In addition, for convenience of numerical calculations the tensor potential is regularized at small distances by the factor

TABLE I. The parameters of the potential of  $\Lambda_c \bar{\Lambda}_c$  interaction.

	$V_S$	$V_D$	$V_T$
$U$ (MeV)	-1025	-156	-64
$R$ (fm)	1.05	1.99	0.78

with  $b = 10 \text{ fm}^{-1}$ . In fact, the results are almost independent of the specific value of the parameter  $b$ .

The parameters of potentials providing the best agreement with experimental data [24,25] for the cross section and for the electromagnetic form factors  $G_E$  and  $G_M$  are given in Table I. Figure 1(a) shows a comparison of the energy dependence of the cross section (7) with experimental data [24,25]. The energy dependencies of  $|G_E/G_M|$  and  $|G_M|$  are shown in Figs. 1(b) and 1(c), respectively. It is seen that our prediction for  $\sigma$ ,  $|G_E/G_M|$  and  $|G_M|$  are in good agreement with experimental data. The corresponding ratio  $\chi^2/N_{df}$  is 1.5, where  $N_{df}$  is the number of degrees of freedom. For the parameters specified in Table I, our model predicts a bound state with energy  $E_0 = -38 \text{ MeV}$ . This bound state may manifest itself in anomalous behavior of light meson production cross sections in  $e^+e^-$  annihilation near  $E_0$  corresponding to  $Q = 4545 \text{ MeV}$  (cf. [31] and references therein).

*Conclusion.* Using the latest BESIII data [24,25] on the cross section of  $\Lambda_c \bar{\Lambda}_c$  pair production in  $e^+e^-$  annihilation and corresponding electromagnetic form factors  $G_E$  and  $G_M$ , analysis of various contributions to the  $\Lambda_c$  and  $\bar{\Lambda}_c$

interaction potential was carried out. The consideration is based on an approach using effective potential. Good agreement was obtained of our predictions with experimental data. Since the ratio  $|G_E/G_M|$  differs significantly from unity in a wide energy region, an account for tensor forces ( $V_T$ ) is crucially important, although  $|V_T| \ll |V_S|$  (see Table I). Note that an account for the potential  $V_D$ , which differs from  $V_S$  due to the spin-orbit interaction, is

also important. Influence of Coulomb interaction is noticeable only in a narrow energy region near the threshold of  $\Lambda_c \bar{\Lambda}_c$  production. We predict existence of a narrow subthreshold resonance in the system  $\Lambda_c \bar{\Lambda}_c$  at energy  $\sim 38$  MeV below the threshold. This bound state may manifest itself in anomalous behavior of light meson production cross sections in a given energy region.

- 
- [1] B. Aubert *et al.*, *Phys. Rev. D* **73**, 012005 (2006).  
 [2] J. P. Lees *et al.*, *Phys. Rev. D* **87**, 092005 (2013).  
 [3] J. P. Lees *et al.*, *Phys. Rev. D* **88**, 072009 (2013).  
 [4] R. R. Akhmetshin *et al.*, *Phys. Lett. B* **759**, 634 (2016).  
 [5] R. R. Akhmetshin *et al.*, *Phys. Lett. B* **794**, 64 (2019).  
 [6] M. Ablikim *et al.*, *Phys. Rev. D* **99**, 092002 (2019).  
 [7] M. N. Achasov *et al.*, *Phys. Rev. D* **90**, 112007 (2014).  
 [8] M. Ablikim *et al.*, *Nat. Phys.* **17**, 1200 (2021).  
 [9] M. N. Achasov *et al.*, *Eur. Phys. J. C* **82**, 761 (2022).  
 [10] M. N. Achasov *et al.*, arXiv:2309.05241.  
 [11] B. Aubert *et al.*, *Phys. Rev. Lett.* **102**, 012001 (2009).  
 [12] R. Mizuk *et al.*, *J. High Energy Phys.* **06** (2021) 137.  
 [13] J. Z. Bai *et al.*, *Phys. Lett. B* **510**, 75 (2001).  
 [14] M. Ablikim *et al.*, *Phys. Rev. D* **80**, 052004 (2009).  
 [15] J. Bai *et al.*, *Phys. Rev. Lett.* **91**, 022001 (2003).  
 [16] M. Ablikim *et al.*, *Eur. Phys. J. C* **53**, 15 (2008).  
 [17] J. P. Alexander *et al.*, *Phys. Rev. D* **82**, 092002 (2010).  
 [18] M. Ablikim *et al.*, *Phys. Rev. Lett.* **108**, 112003 (2012).  
 [19] M. Ablikim *et al.*, *Phys. Rev. D* **87**, 112004 (2013).  
 [20] B. Aubert *et al.*, *Phys. Rev. D* **76**, 092006 (2007).  
 [21] M. Ablikim *et al.*, *Phys. Rev. D* **97**, 032013 (2018).  
 [22] M. Ablikim *et al.*, *Phys. Rev. D* **107**, 072005 (2023).  
 [23] G. Pakhlova *et al.*, *Phys. Rev. Lett.* **101**, 172001 (2008).  
 [24] M. Ablikim *et al.*, *Phys. Rev. Lett.* **120**, 132001 (2018).  
 [25] M. Ablikim *et al.*, arXiv:2307.07316.  
 [26] M. Ablikim *et al.*, *Phys. Rev. D* **104**, 052006 (2021).  
 [27] V. F. Dmitriev and A. I. Milstein, *Phys. Lett. B* **658**, 13 (2007).  
 [28] V. F. Dmitriev, A. I. Milstein, and S. G. Salnikov, *Phys. At. Nucl.* **77**, 1173 (2014).  
 [29] V. F. Dmitriev, A. I. Milstein, and S. G. Salnikov, *Phys. Rev. D* **93**, 034033 (2016).  
 [30] A. I. Milstein and S. G. Salnikov, *Nucl. Phys.* **A977**, 60 (2018).  
 [31] A. I. Milstein and S. G. Salnikov, *Phys. Rev. D* **106**, 074012 (2022).  
 [32] J. Haidenbauer, X.-W. Kang, and U.-G. Meißner, *Nucl. Phys.* **A929**, 102 (2014).  
 [33] X.-W. Kang, J. Haidenbauer, and U.-G. Meißner, *Phys. Rev. D* **91**, 074003 (2015).  
 [34] V. F. Dmitriev, A. I. Milstein, and S. G. Salnikov, *Phys. Lett. B* **760**, 139 (2016).  
 [35] A. I. Milstein and S. G. Salnikov, *Nucl. Phys.* **A966**, 54 (2017).  
 [36] A. I. Milstein and S. G. Salnikov, *Phys. Rev. D* **105**, L031501 (2022).  
 [37] A. I. Milstein and S. G. Salnikov, *Phys. Rev. D* **105**, 074002 (2022).  
 [38] A. I. Milstein and S. G. Salnikov, *JETP Lett.* **117**, 901 (2023).  
 [39] A. I. Milstein and S. G. Salnikov, *Phys. Rev. D* **104**, 014007 (2021).  
 [40] S. G. Salnikov, A. E. Bondar, and A. I. Milstein, *Nucl. Phys.* **A1041**, 122764 (2023).  
 [41] J. Haidenbauer and U.-G. Meißner, *Phys. Lett. B* **761**, 456 (2016).  
 [42] J. Haidenbauer, U.-G. Meißner, and L.-Y. Dai, *Phys. Rev. D* **103**, 014028 (2021).  
 [43] J. Haidenbauer and U.-G. Meißner, *Eur. Phys. J. A* **59**, 136 (2023).  
 [44] S. M. Flatté, *Phys. Lett. B* **63**, 224 (1976).  
 [45] Y. Kalashnikova and A. V. Nefediev, *Phys. Usp.* **62**, 568 (2019).